

A Comparative Conflict Resolution Dataset Derived from Argoverse-2: Scenarios with vs. without Autonomous Vehicles

Guopeng Li^{1,*}, Yiru Jiao^{1,*}, Simeon C. Calvert¹, and J.W.C. van Lint¹

Abstract—As the deployment of autonomous vehicles (AVs) becomes increasingly prevalent, ensuring safe and smooth interactions between AVs and other human agents is of critical importance. In the urban environment, how vehicles resolve conflicts has significant impacts on both driving safety and traffic efficiency. To expedite the studies on evaluating conflict resolution in AV-involved and AV-free scenarios at intersections, this paper presents a high-quality dataset derived from the open Argoverse-2 motion forecasting data. First, scenarios of interest are selected by applying a set of heuristic rules regarding post-encroachment time (PET), minimum distance, trajectory crossing, and speed variation. Next, the quality of the raw data is carefully examined. We found that position and speed data are not consistent in Argoverse-2 data and its improper processing induced unnecessary errors. To address these specific problems, we propose and apply a data processing pipeline to correct and enhance the raw data. As a result, 5k+ AV-involved scenarios and 16k+ AV-free scenarios with smooth and consistent position, speed, acceleration, and heading direction data are obtained. Further assessments show that this dataset comprises diverse and balanced conflict resolution regimes. This informative dataset provides a valuable resource for researchers and practitioners in the field of autonomous vehicle assessment and regulation. The dataset is openly available via https://github.com/RomainLITUD/conflict_resolution_dataset.

Index Terms—Autonomous vehicle, conflict resolution, trajectory processing, trajectory dataset

I. INTRODUCTION

The concept of high-level Autonomous vehicles (AVs) is expected to revolutionize Intelligent Transportation Systems (ITS), offering the promise of safer roads, enhanced mobility, and increased traffic efficiency [1]. Before reaching fully automated traffic, AVs will co-exist with human road users in the foreseeable future. In such a mixed-traffic environment, the incorporation of AVs introduces a novel dimension to the individual interactions between road agents, as well as collective traffic flow characteristics [2]. Interaction between AVs and human road users encapsulates both the control of AVs and the behavioural adjustments of human drivers. These two sides are entwined and thus necessitate a deeper understanding of how human road users re-configure their behaviours to adopt the presence of AVs. This is the foundation for exploring the safety and efficiency impacts of AVs on ITS [3].

For studying how humans react to AVs, large-scale real-world field test data is indispensable. Specifically in urban

traffic, current studies predominantly focus on comparing car-following behaviours in AV-involved trajectory datasets. For example, Hu et al. [4] present an enhanced car-following dataset from the Waymo open data [5]. Their follow-up study finds that there is no significant difference when a human driver (HV) follows an AV compared with following another HV [6]. Using the same dataset, Wang et al. [7] analyze the car-following behaviours approaching signalized intersections and reveal that HVs adapt their behaviours to AVs when decelerating and accelerating. Wen et al. [8] also use the Waymo data and conclude that human drivers exhibit decreased driving volatility, reduced time headways, and increased time-to-collision values when following AVs. Li et al. [9] present another large comparative car-following dataset derived from Lyft level-5 data [10]. These datasets and studies shed light on the possible impacts of AVs on driving safety, efficiency, and string stability of one-dimensional traffic flow.

However, besides car-following, *conflict resolution* at intersections plays an equally if not more, critical role in urban traffic. Intersections re-distribute traffic flow and they are generally efficiency bottlenecks and accident-prone areas [11]. Compared to car-following, vehicle interactions in these conflicted areas are of higher complexity, as they are two-dimensional and sometimes comprise multiple agents. Therefore, evaluating and comparing conflict resolution behaviours for AV-involved and AV-free scenarios becomes an important step towards deploying AVs in mixed-traffic environments and assessing their efficiency impacts. Currently, there is no dataset specifically focusing on conflict resolution with vs. without AVs in the literature. To facilitate such studies on conflict resolution at urban intersections, this paper offers a high-quality and well-classified trajectory dataset derived from the open Argoverse-2 data [12]. The major contributions are summarized below:

- Select AV-involved and AV-free conflict resolution scenarios from Argoverse-2.
- Propose a data processing pipeline to correct and enhance the raw data.
- Classify conflict regimes based on the arrival and departure from the conflict point.

This paper is organized as follows. First, Section.II explains the suitability of Argoverse-2 data and Section.III introduces our methodological framework. Next, scenario selection, raw data assessment, and data enhancement are presented sequentially in Sections IV, V, and VI. Finally, Section.VII assesses the quality of the enhanced dataset and

¹ Department of Transport & Planning, Delft University of Technology, the Netherlands

* Co-first author, equal contribution

TABLE I
COMPARISON OF OPEN AV DATSETS

Properties	Waymo v1.2 [5]	Argoverse-1 [13]	Lyft [10]	Shifts [14]	Nuscenes [15]	Argoverse-2 [12]
AV labelled	✗	✓	✓	✗	✓	✓
Autonomous mode	✓	?	✓	?	✗	✓
Conflict resolution	✓	✓	✗	✗	✗	✓
Track duration (s)	9	5	300+	10	8	11
Frequency (Hz)	10	10	10	5	2	10

classifies conflicts into 9 regimes for users.

II. DATASET SELECTION AND DESCRIPTION

To derive a conflict resolution dataset that comprises both AV-involved and AV-free scenarios, a proper data source meeting the following requirements is necessary:

- AVs must be labelled.
- The AV's autonomous mode must be on.
- The conflict resolution cases at intersections should be diverse.
- The tracking duration should be long enough to cover the entire conflict resolution process.
- The sampling frequency should be high enough to provide behavioural details.

Table I compares 6 popular open motion datasets. The recently-released Argoverse-2 [12] motion forecasting dataset fulfils all these requirements. Argoverse-2 is collected by an automated fleet in 6 cities. The dataset contains 250k selected non-overlapping scenarios specifically focused on safety-critical long-tailed situations. The duration of each scenario is 11s with a uniform 10Hz sampling rate (0.1s time interval). Elements of high-definite maps, including vectorized maps and drivable areas, are also provided. For each road agent, timestamps, positions, velocities, and heading (yaw) directions are provided in the raw data. The developers also provide a Python toolkit "av2-api" ¹ to read, process, and visualize the data.

In this paper, we aim to extract, assess, enhance, and classify the AV-involved and AV-free conflict resolution cases from the Argoverse-2 motion forecasting dataset. Next, we will present the methodological framework.

III. METHODOLOGICAL FRAMEWORK

Fig. 1 shows the framework of this study, which contains 4 major parts. Firstly, conflict resolution scenarios are selected based on a set of rules. Next, the data quality of the raw trajectories is assessed. Then, we propose a trajectory correction and smoothing pipeline to enhance the raw data. Maps are also re-processed for user-friendliness. Finally, the quality of the enhanced data and the diversity of conflict regimes in the obtained dataset are evaluated. We will introduce each step in detail in the following sections.

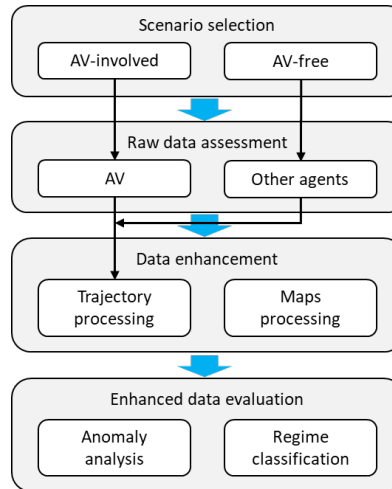


Fig. 1. Framework of the data preparation and evaluation process.

IV. SCENARIO SELECTION

We start by selecting conflict resolution scenarios. First of all, it is necessary to clarify what the so-called "conflict" is in this study. In general, a conflict refers to a situation in which two or more road agents create a risk of collision, disruption, or interference with each other's intended paths or movements. In this paper, we focus on a very specific type of conflict: *One vehicle (AV or HV) and another road agent with different coming lanes and different intended lanes pass the same location sequentially*. Most of these types of conflicts occur at intersections and T-junctions. Lane-changing and other conflicts are not considered in this paper.

Based on clarifying the conflicts of interest, we set 4 heuristic rules to select desired scenarios:

- The two trajectories must cross each other to exclude car-following, merging, lane-changing, etc.
- The two agents have a short minimum distance or pass the same location (conflict point) in a short time interval.
- At least one of the two agents changes its behaviour before passing the conflict point.

For applying the first rule, we use the method presented in Fig. 2. For each of the two trajectories, two parallel buffer curves with distances to the trajectory of d are added. One trajectory must intersect both buffer curves of the other, to be considered as crossing. We set $d = 3$ m (approximately the width of a lane) for vehicles. For vulnerable agents such

¹<https://github.com/argoverse/av2-api>

as pedestrians and cyclists, $d = 1.5$ m. This "trick" of buffer curves can effectively exclude undesired conflict types.

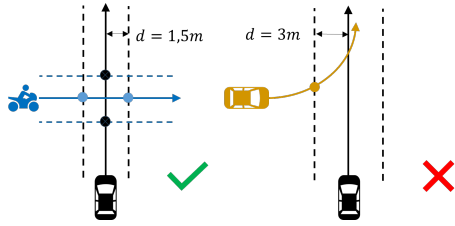


Fig. 2. Illustration of identifying crossing trajectories.

For the second rule, we set a critical minimum distance of 8 m between the centroids of two agents. We also utilise a surrogate safety metric, the so-called Post-Encroachment-Time (PET). PET refers to the time difference between an encroaching road agent leaving the conflict area and another road agent entering the same area. A threshold is needed to distinguish serious conflicts from non-serious conflicts. According to Peesapati et al. [16], 1.5 s is a reasonable value in unprotected left-turn cases. However, serious conflicts are rare in practice and most serious conflicts are resolved before happening. Another concern is that ArgoAI AVs may drive more conservatively than human drivers. Therefore, this threshold is relaxed to 5 s for scenario selection. Note that there are various approaches to calculating PET, for example, defining the conflict area as a reference. In this study, considering the diversity of intersection layouts, we use the crossing point of the trajectories as the anchor (conflict point). Consequently, we exclude those scenarios with $PET > 5$ s and a minimum distance > 8 m.

The third rule poses additional constraints. First, at least one of the agents must move a distance longer than 8 m to avoid tacking fluctuations induced by sensors. Second, if PET is larger than 3 s, then at least one of the conflicting agents must have a speed variation larger than 3 m s^{-1} before arriving at the conflict point. The underlying assumption is that, for such a large PET, if neither of the agents brake or accelerate, there is no conflict resolution at all.

After applying all these 3 rules, we obtain the selected scenarios and conflicting agents. Fig.3 shows the type distributions of agents conflicting with an AV or an HV. Most of the conflicts happen between two vehicles. Conflict resolution can take other road agents into account, even if their trajectories do not intersect with the conflicting agents. It is thus necessary to include road agents surrounding the conflict point. To do so, we draw a circle with the radius of 30 m around the conflict point to include all agents whose trajectories intersect with the circle or are completely inside it. As the final result, the number of selected scenarios and the average number of surrounding agents are listed in Table.II. Next, we will assess the quality of the raw data in Argoverse-2.

V. RAW DATA ASSESSMENT

The motion data of the AVs and of the surrounding agents were obtained in different ways. For AVs, their positions

TABLE II
SELECTED SCENARIOS FROM ARGOVERSE-2

Category	Nb. of scenarios	Average Nb. of agents
AV-involved	5337	20.5
AV-free	16094	21.7

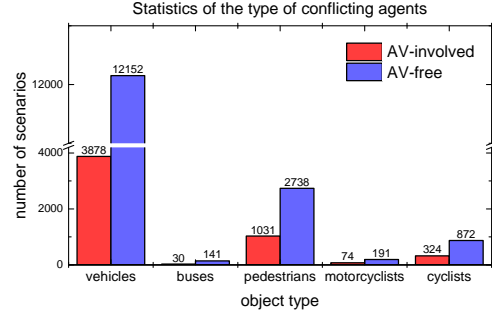


Fig. 3. Distributions of different types of conflicting agents

and speeds can be directly reconstructed from the CAN bus records. However, the motion of surrounding agents is usually processed from perception data, e.g. camera and LiDAR. Therefore, it is necessary to assess the quality of the trajectories separately for AVs and other agents. The raw data provide the location (x, y) , speed (v_x, v_y) , and heading ϕ for each non-static agent. In this subsection, we mainly examine the consistency between positions and speeds.

The speed derived from position series, for example at moment t , is:

$$v_p = \frac{s_{t-1,t} + s_{t,t+1}}{2\Delta t} \quad (1)$$

$$s_{t-1,t} = \sqrt{(x_t - x_{t-1})^2 + (y_t - y_{t-1})^2}$$

We call this *position-based speed*. In Fig.4, the position-based speed is compared with the given speed for 4 different types of agents in one of the selected scenarios. The comparison shows that the raw data in Argoverse-2 are not internally consistent. This inconsistency is observed for every non-static trajectory in Argoverse-2.

We can observe that the first and the last 1-1.5 s of the position series are not correctly processed. For all trajectories, position-based speed has a significantly sharp drop at the beginning and the end of each scenario. The drop magnitude is always half of the nearest peak value. This type of error can be produced by improper processing methods, such as fitting a polynomial with boundary constraints or using over-fitted wavelet denoising smoothers. In Fig.5, we further quantify the inconsistency of speed and trajectory length, respectively. The left figure shows that the first and the last 1.5 s of the trajectories have significantly higher MAE (between the given speed and the position-based speed). In the middle time period of each scenario, AV's speed and position are highly consistent but other agents have significantly lower consistency. The right plot of Fig.5 presents the distribution of trajectory length inconsistency, which is the difference

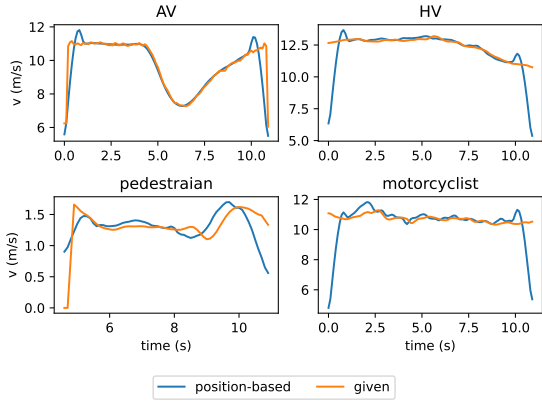


Fig. 4. Comparison of the given speed and the position-based speed for 4 different types of agents.

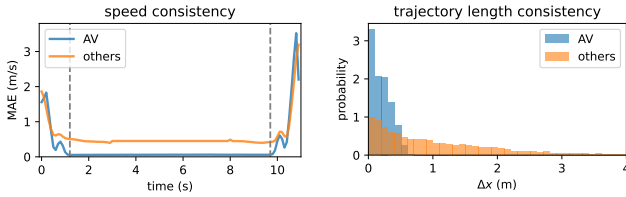


Fig. 5. The consistency between the given speed and the position-based speed (left) and the lengths of given trajectories and the trajectories reconstructed from the given speed (right). AVs and other agents are plotted respectively.

in travelling distance between the given trajectory and the trajectory constructed from the given speed by numerical integration. For AVs, the difference is always smaller than 0.6 m. But for other agents, the difference has a fat-tailed distribution. This inconsistency is problematic for further analysing the driving behaviours in detail.

It is noticed that the given speed series are noisier than the position-based speed series, especially for AVs. For other agents, some missing speed data was filled by 0 (this is also reported in Lyft level-5 data [9]). Compared with position-based speed, the given speed does not have strange drops but only the isolated outlier induced by 0-value padding. Therefore, we infer that *the provided speed is more reliable than positions*. This is the basic assumption for the following data enhancement.

VI. DATA ENHANCEMENT

As pointed out in the previous section, the raw data of Argoverse-2 cannot be directly used due to significant inconsistency. This section describes how we correct and enhance the raw data, including both the trajectories and the vectorized maps.

A. Trajectory processing

The flowchart of trajectory processing is presented in Fig. 6. AVs and non-AV agents share the same procedure but are processed differently after speed correction.

The first step is speed outlier correction. At moment t , the speed $v(t)$ is an outlier if the acceleration is abnormally high

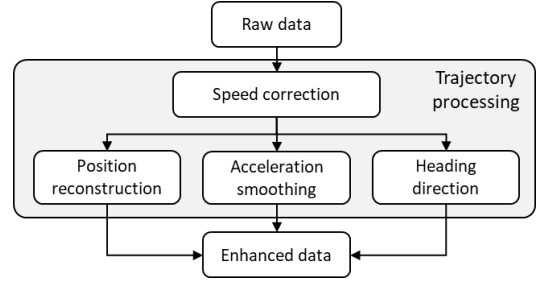


Fig. 6. Trajectory processing and enhancement.

or any speed in the neighbouring time interval is filled with 0:

$$\begin{aligned} & \left| \frac{dv(t)}{dt} \right| > 10 \text{ m s}^{-2} \quad \text{or} \\ & \exists t' \in [t - 0.3 \text{ s}, t + 0.3 \text{ s}], \text{ s.t. } v(t') = 0 \end{aligned} \quad (2)$$

To correct these outliers, we simply assume that the jerk is constant along both directions of x and y , which means that $v_x(t)$ and $v_y(t)$ are parabola (2nd-degree polynomial). This local parabola is fitted from the nearest 1 s window observation and then used to replace the outliers. Because most of the outliers are isolated points or a short segment less than 0.3 s, this approximation will not induce large errors. The corrected speed is noted as $v'(t)$.

The second step is position reconstruction. For AVs, the first and the last 1.5 s of the position series are reconstructed from the corrected speed. For example, when reconstructing the last 1.5 s, we denote the initial x -position as x_0 , and derive new x -positions after T by:

$$x(T) = x_0 + \int_0^T v'_x(t) dt \quad (3)$$

The integration here can be numerically computed by Simpson's rule [17] and the same formula can be used for y -positions as well. For non-AV agents, because their position and speed are inconsistent throughout the entire trajectory, we have to completely reconstruct the position data. We maintain the main trend of the given position but re-segment the trajectory based on minimising the change in corrected speed within each segment. First, the average speed of each time interval is computed. Next, the trajectory is re-segmented based on the polyline of average speeds along time. These segment points are where the new position data are reconstructed. However, not all lost information can be retrieved in this way. For the following situations, we do not correct trajectories but preserve the raw data:

- The duration is shorter than 5 s. The unreliable percentage is too high so we cannot correct the data.
- The length of the trajectory is shorter than 5 m. The perception fluctuation is too large.
- The trajectory length inconsistency is larger than 2 m.

Next, the corrected speed is smoothed, from which we derive acceleration and heading direction. For AVs, considering that the speed is noisy, we use the wavelet denoise method [18] to smooth the speed and derive acceleration by

computing gradient. Here we use the wavelet denoising in `skimage` python package. The noise is set to $\sigma = 0.5 \text{ m s}^{-1}$ (by trial-and-error). The wavelet mode is the Daubechies family with 6 vanishing moments ('db6'). The soft threshold method is used and the maximum wavelet decomposition level is 3. For non-AV agents, the corrected speed is smooth enough already, so we directly compute the gradient as acceleration. The heading is defined as the tangent direction of the trajectory. Because the bounding boxes of vehicles are not given in the raw data, we cannot further process the yaw direction.

As an example, Fig.7 compares the raw and the processed motion data for an AV and an HV in the case of an unprotected left turn. The outliers are removed. The speed and acceleration are smoother after processing.

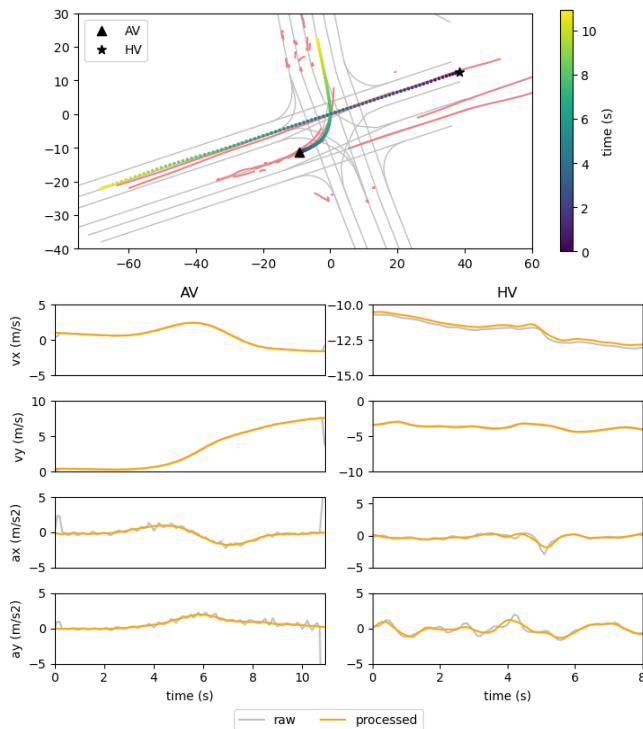


Fig. 7. Example of comparison between raw and processed motion data.

B. Vectorized maps processing

Argoverse-2 provides vectorized lane geometries along the driving direction. The average length of all lane segments is around 15m, so there are too many segments contained in each scenario. To save storage space and preserve road connectivity and traffic rules, we combine and merge the lane segments by the following rules:

- Segments are merged together if one is the only down-stream segment of the other one.
- All combined lanes start and end at the boundary of the maps, a diverging point, or a merging point.
- All combined lanes are re-segmented into a series of 20 tail-to-head vectors along the driving direction.

Using these rules, road maps can be stored in a compact array and the adjacency matrix of all combined lanes can be easily constructed through indexing the start/end positions. Two examples of the processed maps are shown in Fig.8. Different colours represent different segments of lanes. The arrow at the end of each segment indicates the driving direction.

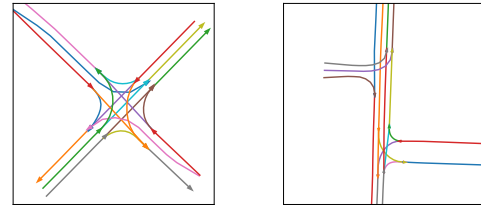


Fig. 8. Two examples of processed vectorized maps.

By far, we have introduced the complete data selection and enhancement procedure.

VII. ENHANCED DATA EVALUATION

With the dataset obtained, now we focus on evaluating its quality and the diversity of conflict resolution processes included.

A. Anomaly analysis

In addition to speed inconsistency introduced in Section V, we consider 3 constraints on acceleration a and jerk j proposed by Punzo et al. [19] to assess data quality:

- $a \in [-8, 5] \text{ m/s}^2$
- $j \in [-15, 15] \text{ m/s}^3$
- The jerk's sign cannot reverse more than once in 1s (*Jerk Sign Inversion, JSI*).

Violating any of these constraints is considered to be an “anomaly”. Table.III presents the speed inconsistency (Δv) and the time percentages of detected anomalies of acceleration, jerk, and JSI. The enhanced data is compared with the raw data. The result shows that the quality of the enhanced data is indeed significantly improved compared to the raw data in Argoverse-2.

TABLE III
ANOMALY ASSESSMENT

Dataset	$\Delta v \text{ (m s}^{-1}\text{)}$	acc %	jerk %	JSI %
AV-enhanced	0.01	0.01	0.01	0.3
Others-enhanced	0.30	0.01	0.03	0.9
AV-raw	0.32	0.21	0.23	83.6
Others-raw	3.30	0.14	0.19	13.9

B. Regime classification

Next, we evaluate the diversity of selected scenarios. Conflict regimes in the scenarios are classified based on the relative movement of the two vehicles, i.e., whether they run parallel (P), cross (C), or run opposite (O) to each other before and after reaching the conflict point. Consequently, there are 9 combinations as shown in Fig. 9. Further, we differentiate these combinations by considering whether the second-passing vehicle was from the left or the right of the first-passing vehicle. For simplification, we use a notation of two letters pointed by an arrow to represent these cases. For example, $\mathbf{P} \rightarrow \mathbf{C}$ indicates that the two vehicles were running parallel before the conflict point and crossing afterwards, and the second-passing vehicle moved from the left to the right of the first-passing vehicle.

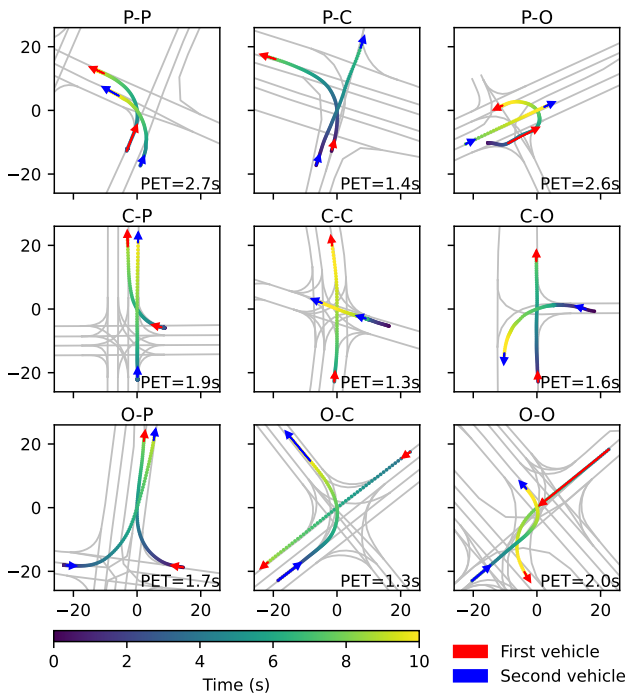


Fig. 9. Nine combinations of conflict regimes

We consider 3 types of scenarios to observe the distribution of these regimes. (1) An AV passing the conflict point before an HV (*AV-first*); (2) an AV passing the conflict point after an HV (*AV-second*); (3) AV-free scenarios. In Fig. 10, we present the statistics of vehicle-vehicle conflicts in the 3 types of scenarios, showing similar regime distributions across them. Around and more than 80% conflicts fall into $\mathbf{O} \rightarrow \mathbf{C}$ and $\mathbf{C} \rightarrow \mathbf{C}$. Among the regimes, $\mathbf{O} \rightarrow \mathbf{C}$ is the most common, and unprotected left turns belong to it. The result shows that the dataset contains diverse and balanced conflict regimes for both AV-involved and AV-free scenarios.

The distributions of PET of the 3 types of scenarios are further shown in Fig. 11. AV-first and AV-free scenarios have similar PET distributions, while AV-second scenarios have a significantly different PET distribution with a higher average. This comparison implies two things. First, the AVs

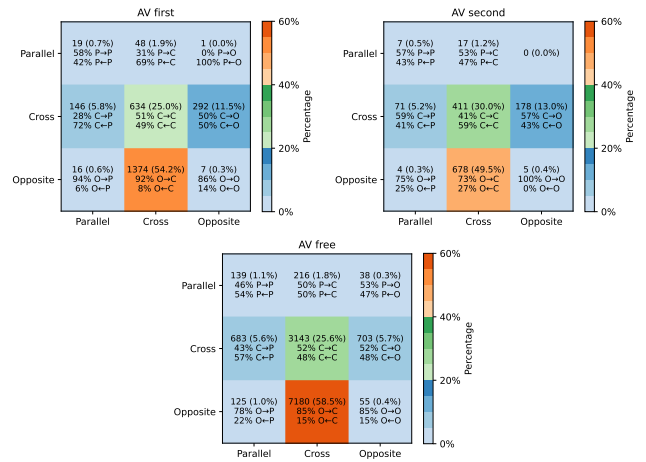


Fig. 10. Statistics of conflict regimes for different scenarios.

in Argoverse-2 data drove more conservatively than human drivers in general. They tended to preserve for a longer time to avoid potential conflicts. Second, averagely speaking, when human drivers pass conflict points after AVs, they do not behave differently compared with interacting with an HV. Nevertheless, these observations require deeper investigation.

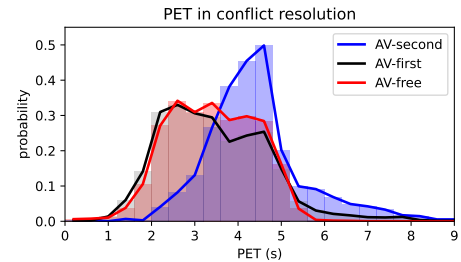


Fig. 11. Distributions of PETs in different scenarios.

VIII. CONCLUSION

In this paper, we present a comparative conflict resolution dataset comprising diverse and balanced AV-involved and AV-free scenarios. The raw trajectories provided by Argoverse-2 are carefully examined, corrected, and enhanced. The enhanced data are of higher quality than the raw data and diverse conflict resolution regimes are covered in the scenarios. This dataset is valuable for multiple domains, such as optimizing interactive behaviours of AVs and evaluating the efficiency and safety impacts of AVs.

ACKNOWLEDGMENT

This research is sponsored by the NWO/TTW project MiRRORS with grant agreement number 16270 and the TU Delft AI Labs programme. We thank them for supporting this study.

REFERENCES

- [1] F. Duarte and C. Ratti, "The impact of autonomous vehicles on cities: A review," *Journal of Urban Technology*, vol. 25, no. 4, pp. 3–18, 2018.

- [2] H. Yu, R. Jiang, Z. He, Z. Zheng, L. Li, R. Liu, and X. Chen, "Automated vehicle-involved traffic flow studies: A survey of assumptions, models, speculations, and perspectives," *Transportation research part C: emerging technologies*, vol. 127, p. 103101, 2021.
- [3] Q. Lu, T. Tettamanti, D. Hörcher, and I. Varga, "The impact of autonomous vehicles on urban traffic network capacity: an experimental analysis by microscopic traffic simulation," *Transportation Letters*, vol. 12, no. 8, pp. 540–549, 2020.
- [4] X. Hu, Z. Zheng, D. Chen, X. Zhang, and J. Sun, "Processing, assessing, and enhancing the waymo autonomous vehicle open dataset for driving behavior research," *Transportation Research Part C: Emerging Technologies*, vol. 134, p. 103490, 2022.
- [5] P. Sun, H. Kretschmar, X. Dotiwala, A. Chouard, V. Patnaik, P. Tsui, J. Guo, Y. Zhou, Y. Chai, B. Caine, *et al.*, "Scalability in perception for autonomous driving: Waymo open dataset," in *Proceedings of the IEEE/CVF conference on computer vision and pattern recognition*, pp. 2446–2454, 2020.
- [6] X. Hu, Z. Zheng, D. Chen, and J. Sun, "Autonomous vehicle's impact on traffic: empirical evidence from waymo open dataset and implications from modelling," *IEEE Transactions on Intelligent Transportation Systems*, 2023.
- [7] Y. Wang, H. Farah, R. Yu, S. Qiu, and B. van Arem, "Characterizing behavioral differences of autonomous vehicles and human-driven vehicles at signalized intersections based on waymo open dataset," *Transportation Research Record*, p. 03611981231165783, 2023.
- [8] X. Wen, Z. Cui, and S. Jian, "Characterizing car-following behaviors of human drivers when following automated vehicles using the real-world dataset," *Accident Analysis & Prevention*, vol. 172, p. 106689, 2022.
- [9] G. Li, Y. Jiao, V. L. Knoop, S. C. Calvert, and J. van Lint, "Large car-following data based on lyft level-5 open dataset: Following autonomous vehicles vs. human-driven vehicles," *arXiv preprint arXiv:2305.18921*, 2023.
- [10] J. Houston, G. Zuidhof, L. Bergamini, Y. Ye, L. Chen, A. Jain, S. Omari, V. Iglovikov, and P. Ondruska, "One thousand and one hours: Self-driving motion prediction dataset," in *Conference on Robot Learning*, pp. 409–418, PMLR, 2021.
- [11] Á. Briz-Redón, F. Martínez-Ruiz, and F. Montes, "Spatial analysis of traffic accidents near and between road intersections in a directed linear network," *Accident Analysis & Prevention*, vol. 132, p. 105252, 2019.
- [12] B. Wilson, W. Qi, T. Agarwal, J. Lambert, J. Singh, S. Khandelwal, B. Pan, R. Kumar, A. Hartnett, J. K. Pontes, *et al.*, "Argoverse 2: Next generation datasets for self-driving perception and forecasting," *arXiv preprint arXiv:2301.00493*, 2023.
- [13] M.-F. Chang, J. Lambert, P. Sangkloy, J. Singh, S. Bak, A. Hartnett, D. Wang, P. Carr, S. Lucey, D. Ramanan, *et al.*, "Argoverse: 3d tracking and forecasting with rich maps," in *Proceedings of the IEEE/CVF conference on computer vision and pattern recognition*, pp. 8748–8757, 2019.
- [14] A. Malinin, N. Band, G. Chesnokov, Y. Gal, M. J. Gales, A. Noskov, A. Ploskonosov, L. Prokhorenkova, I. Provilkov, V. Raina, *et al.*, "Shifts: A dataset of real distributional shift across multiple large-scale tasks," *arXiv preprint arXiv:2107.07455*, 2021.
- [15] H. Caesar, V. Bankiti, A. H. Lang, S. Vora, V. E. Liong, Q. Xu, A. Krishnan, Y. Pan, G. Baldan, and O. Beijbom, "nusenes: A multimodal dataset for autonomous driving," in *Proceedings of the IEEE/CVF conference on computer vision and pattern recognition*, pp. 11621–11631, 2020.
- [16] L. N. Peesapati, M. P. Hunter, and M. O. Rodgers, "Evaluation of postencroachment time as surrogate for opposing left-turn crashes," *Transportation research record*, vol. 2386, no. 1, pp. 42–51, 2013.
- [17] L. N. G. Filon, "Iii.—on a quadrature formula for trigonometric integrals," *Proceedings of the Royal Society of Edinburgh*, vol. 49, pp. 38–47, 1930.
- [18] Q. Pan, L. Zhang, G. Dai, and H. Zhang, "Two denoising methods by wavelet transform," *IEEE transactions on signal processing*, vol. 47, no. 12, pp. 3401–3406, 1999.
- [19] V. Punzo, M. T. Borzacchiello, and B. Ciuffo, "On the assessment of vehicle trajectory data accuracy and application to the next generation simulation (ngsim) program data," *Transportation Research Part C: Emerging Technologies*, vol. 19, no. 6, pp. 1243–1262, 2011.